Least square inversion with time shift optimization and an application to earthquake source mechanism

L. R. Jordanovski

Institute of Earthquake Engineering and Engineering Seismology, Skopje, Yugoslavia

M. D. Trifunac

Department of Civil Engineering, University of Southern California, Los Angeles, California 90089-2531, USA

A common problem in inversion which involves fitting of the recorded data by some model time series is the lack of knowledge of the absolute time of the recordings. This results in errors in the relative timing between the calculated and the recorded data. Such errors are present, for example, in the inversion of the earthquake source mechanism in terms of the recorded accelerograms.

In this paper a method for optimizing the choice of the relative timing between theoretical and the recorded time history is presented. This highly nonlinear problem is solved by splitting it into two least square problems (LSQ) and by using the method of optimized exhaustive search. The method is illustrated by the inversion of the data for the 1979 Imperial Valley earthquake. It is shown that major differences exist between the results of the inversion with and without time shifting optimization. While the method is illustrated on the problem of the earthquake source inversion, the procedure presented here can be directly applied to many other identification problems involving fitting of the time histories in many vibration or wave propagation problems.

1. INTRODUCTION

The work on a three-dimensional dislocation model for the San Fernando, California, earthquake of February 9, 1971[17], initiated the research in the field of detailed earthquake source inversion using the near-field strong motion data. This first spatial inversion over the fault surface, although very simple, has uncovered wide possibilities for this work and has pointed out to some problems in applicability and in the usefulness of the source inversion studies with strong motion data. There were two main reasons for this. The first one was the overall complexity of the problem and its mathematical modelling involving the earthquake source and the wave propagation problem through the surrounding inhomogeneous medium. The second problem was associated with the lack of the near field data, and other independent but detailed observations required to check the inversion results and hence to prove the theoretical and the practical possibilities of the earthquake source inversion. Many other investigators have also studied the earthquake source mechanism using the strong motion data but with the forward theoretical simulations with essentially 'trial and error' procedures to find the 'best' source mechansim and fitting the recorded data.

In the following years more strong motion data has been collected thus improving the opportunities for further and more detailed research of the earthquake source mechanism[19]. The Imperial Valley earthquake in 1979 was one of the most fruitful contributors in terms of the recorded near-source ground acceleration data and other observations[8]. This earthquake has been subjected to exhaustive research by many researchers focusing on the inversion of its source[1,5,6,9,12], who presented faulting models and the synthetics of the strong motion time histories.

The objective of this paper is to analyze further one specific problem which arises in the source inversion. This is a problem of relative timing between the theoretical and the recorded data or as it will be called here the time shifting error. In the above mentioned papers, this type of error has been pointed out and it has been investigated, and in some cases included in the source inversion model. However, no one has so far presented a method of solution for eliminating this type of error or for its reduction through some optimization algorithm.

In what follows we give a short introduction about the source inversion modelling with special attention to the problem of the time shifting error, and a brief review of the previous work that in some sense has touched on this problem.

2. FORMULATION OF THE INVERSION PROBLEM

The main objective of the source inversion problem is determination of some earthquake source parameters from the analysis of a finite number of recorded strong motion data (acceleration, velocity or displacement). Based on the body force equivalent representation[11,2] a displacement at a point $\vec{x}$, due to discontinuity in the

As communicated by M. D. Trifunac.
Paper received October 1988. Discussion ends February 1991.

© 1990 Computational Mechanics Publications

displacement across the fault surface Σ is given by:

$$u_n(\vec{x},t)=\int_{-\infty}^{-\infty} \mathrm{d}\tau \int_{\Sigma} a_i(\vec{\xi},\tau)K_{in}(\vec{x},\vec{\xi},t-\tau)\,\mathrm{d}\Sigma \qquad (1)$$

where

$$K_{in}(\vec{x},\vec{\xi},t-\tau)=C_{ijpq}n_j(\vec{\xi})\frac{\partial}{\partial\xi_q}G_n^p(\vec{x},\vec{\xi},t-\tau) \qquad (2)$$

is the kernel of integral equation (1). The quantity $u_n(\vec{x},t)$ is the nth component of displacement at the point $\vec{x}$ and at time t due to the ith component of the dislocation vector $\vec{a}(\vec{\xi},t)$, defined over fault surface Σ. $G_n^p(\vec{x},\vec{\xi},t)$ is dynamic Green-tenzor, $n_j(\vec{\xi})$ unit vector of the fault normal and C_{ijpq} the elasticity tenzor. Knowing the left side of equation (1) and solving for the unknown vector function $\vec{a}(\vec{\xi},t)$, the inverse problem is solved. However, practical realization is not so straightforward and one is faced with many problems. Depending on *a priori* knowledge about the faulting process and the computational difficulties the simplifying assumptions are often made about:

(a) dislocation vector $\vec{a}(\vec{\xi},t)$,
(b) geometry of the fault, and
(c) dynamic Green-tenzor.

In general there are four basic parameters that must be specified everywhere on the fault plane to describe the dislocation vector: (a) temporal behaviour of the dislocation, (b) rupture velocity or more generally the time when the dislocation starts at some point, (c) the dislocation rise time (the time required for the dislocation to reach final value) and (d) the rake (direction) of the vector $\vec{a}(\vec{\xi},t)$.

Geometry of the fault is usually defined by four parameters: (a) length, (b) width, (c) strike angle and (d) dip angle. With these parameters it is *a priori* assumed that a plane represents an acceptable geometric description of the fault[12,6,1,9] or a combination of the planes to fit more complex fault geometry[17].

Finally, in the calculation of the dynamic Green–tenzor, one has to make certain simplifications depending on the quality of the information and the data about the geological structure of the surrounding medium. Hence in the literature one can find the Green-tenzor for layered viscous half space[12,6,1] as well as the simplified models of the full and half space[17,9]. In some instances the layered half space model may lead to more realistic representation of the geologic medium, while in other cases it cannot be justified and the simple half or full space models may be preferable. Since the real earth is highly irregular in the three-dimensional sense, particularly for the distances and the wavelengths (frequencies) considered in strong motion seismology, the proper balance between the complexity of the geologic model and of the implied resolution of the overall analysis should be selected. Only those refinements which uniquely contribute to the higher resolution of the end result should be included in the model.

3. METHOD OF SOLUTION

After all necessary parametrization has been completed the selected unknown quantity is the spatial distribution of the dislocation along the fault, or more precisely, the final offset of the dislocation time history. In this case study the Haskell ramp is used for the temporal shape of the dislocation equation (3)[7,17]

$$\vec{a}(\vec{\xi},\tau)=\begin{cases}0 & t<T(\vec{\xi})\\ \dfrac{\vec{D}(\vec{\xi})t}{\tau(\vec{\xi})} & T(\vec{\xi})<t<T(\vec{\xi})+\tau,\\ \vec{D}(\vec{\xi}) & T(\vec{\xi})+\tau<t\end{cases} \qquad (3)$$

where the final offset $\vec{D}(\vec{\xi})$, rise time $\tau(\vec{\xi})$ and, $T(\vec{\xi})$ the time when the rupture starts to grow at point $\vec{\xi}$ are the functions of the position on the fault, $\vec{\xi}$. In the examples presented here we assume that the rise time is constant for all parts of the fault and the rupture arrival time is defined by the constant rupture velocity. Therefore, the unknown vector $\vec{D}$ represents the dislocation offset amplitudes at different points of the fault. We consider only the shear type of rupture with two components of dislocation. To achieve the satisfactory resolution, the fault is divided into N columns. This approach was used for the first time by Trifunac[17] and subsequently in many other inversions[12,6,1]. For each subfault element, the theoretical displacement at an observation point P, due to unit dislocation in the ξ_1 and ξ_2 directions (Fig. 1) is calculated by solving the forward problem. A linear combination of the contributions from the dislocations D_1 in the ξ_1 direction and D_2 in the ξ_2 direction of all subfaults will lead to the total theoretical response. To estimate the actual values of the coefficients in the data the least square error criterion is used for finding unknown dislocations D_1 and D_2. The numerical model will result in a system of linear equations of the form

$$A^T A\vec{D}=A^T\vec{f}. \qquad (4)$$

The system of equation (4) is obtained by minimization of the square error with respect to unknown vector $\vec{D}=(D_1,D_2\ldots D_J)$[17,12,5] or:

$$\min_{\vec{D}} E(\vec{D})=\min_{\vec{D}}\sum_i \int_0^T \left[f_i(t)-\sum_{j=1}^{J}\phi_{ij}(t).D_j\right]^2 \mathrm{d}t \qquad (5)$$

where

$$\phi_{ij}(t) \qquad i=1,2,\ldots,I; \qquad j=1,2,\ldots,2K=J \qquad (6)$$

represent the theoretical displacements obtained from the jth unit dislocation at the ith recording site. Here I is the total number of recorded time histories (three components per station), K is the number of subfaults, and

$$f_i(t), \qquad i=1,\ldots I \qquad (7)$$

represent the recorded displacement data.

Solution of equation (5) leads to the normal equations (4) where the elements of matrix $A^T A$ are given by

$$[A^T A]_{jk}=\int_0^T \phi_{ij}(t)\phi_{ik}(t)\,\mathrm{d}t \qquad \begin{matrix}k=1,\ldots J\\ j=1,\ldots J\end{matrix}$$

and

$$[\vec{f}]_j=\int_0^T \phi_{ij}(t)f_i(t)\,\mathrm{d}t \qquad (8)$$

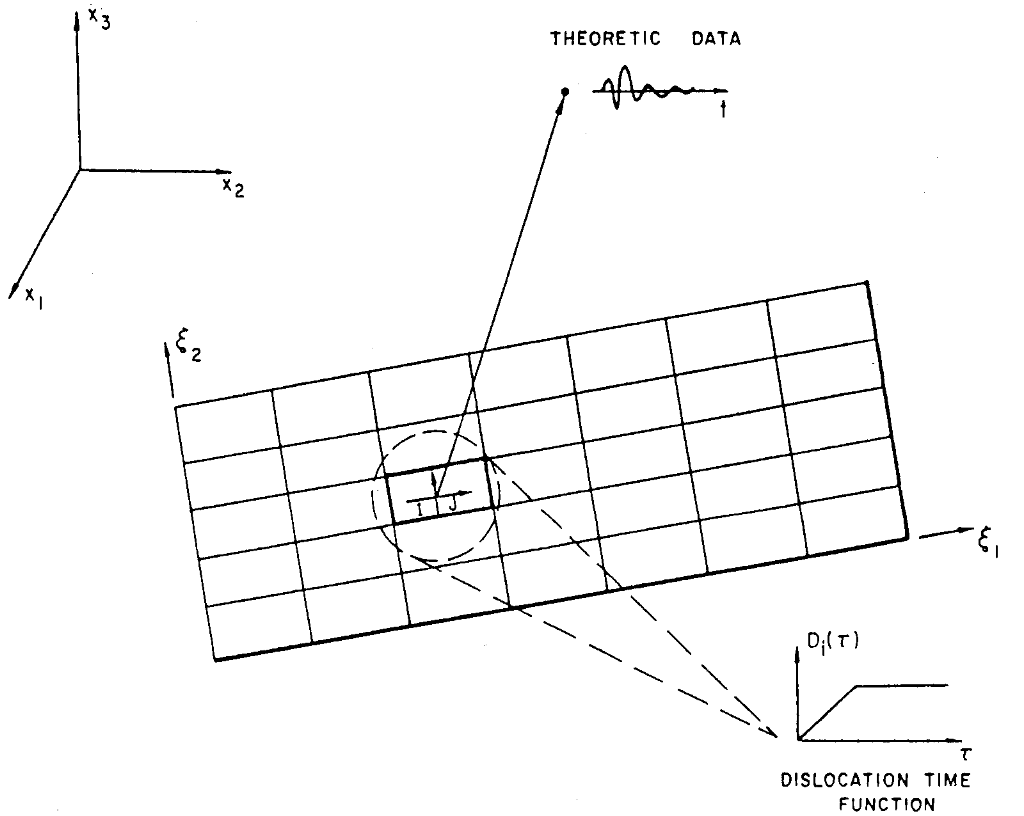

Fig. 1. Illustration of the subfaults, rupture function and the theoretical data used to form the LSQ model

If in the numerical integration of equations (8) the time step is taken equal and the functions $\phi_{ij}(t)$ and $f_i(t)$ are represented by their sample values, then equation (4) originates from the LSQ problem

$$A\vec{D}=\vec{f}. \tag{9}$$

Equation (9) requires that at each discrete time the theoretical displacement be equal to the recorded time function. Since the number of time points may be large, in practice, equation (9) is overdetermined and unstable. The ill-conditioned nature of the system (9) requires attention and special methods for solving it. Since the full treatment of the numerical solution of equation (9) is beyond the scope of this work, the reader is referred to Jordanovski *et al.*[9] and the paper by Olson and Apsel[12], where the method of damped least square is used to solve equation (9). One important source of errors which makes this inversion problem even more ill-posed is the time shifting-error. In the following we consider this type of error in more detail.

STATEMENT OF THE PROBLEM FOR THE TIME SHIFT OPTIMIZATION

The LSQ model in equation (9) is formed by equating the theoretical with the recorded data at the same time coordinates. However, in practice one may not be able to meet this requirement. Most recorded strong motion data, used in the source inversion, usually do not have absolute time[14]. Even if one knew how to obtain the absolute recording time one would still not know precisely the starting time of shaking. The reasons for this can be found in the features of strong motion instruments[14–16,18] and in the complex velocity structure between the source and the recording station. In contrast to the seismological instruments which record continuously, the strong-motion instruments have relatively high trigger levels. Therefore, when an instrument starts recording it is usually not recording the very first strong-ground motion. On the other hand, the calculation of the theoretical data is a controlled process and one is able to define the exact time of all arrivals at a station. So if the first motion is used as a reference point in the LSQ fitting and to form the system (9), an error, which is difficult to estimate is introduced.

One procedure to reduce this time shifting error, could be to begin by first estimating the reference time of each record. That reference point could be, for example, the first arrival of the *S*-waves, which are often identifiable on most strong motion records. Attempts to reduce the effects of this time shifting error have been made by several researchers. Hartzell and Heaton in their paper, dealing with inversion of the Imperial Valley data, have obtained significantly better fitting with a small time shift of synthetic data for four records. They used shift no greater than 1 sec. Since they have not presented the method of solution for the unknown time shift one can assume that their approach consisted of testing several models with different relative timing and starting from the very beginning of the inversion process. Archuleta has associated the time shifting error with the rupture time or with the time when the rupture starts at the same point on the fault. Clearly the rupture time here is nonlinearly related to the synthetics, and through his parametric investigation, he has concluded that the parametrization of the nonlinear variables becomes a very critical element in the process of inversion. Archuleta did not give any solution for this problem, but he stressed that 'because of the importance of the rupture time to the synthetics, an inversion method tailored to determine the rupture time should be developed'. Olson and Apsel suggested one method to handle this problem. They allowed each fault cell to slip five times with sequential time delays, centred on the time when the rupture front arrived at the centre of the cells. In the resulting LSQ model the amplitude of each slip is thus considered as an independent unknown. In this way the number of unknowns is increased five times, which clearly has an offset in the numerical stability of the solution. Though it has different physical meaning, this approach has a numerical advantage over the method of Hartzel and Heaton since the LSQ model is solved only once, but the meaning of the time delays is different. Olson and Apsel essentially model the changes in the rupture propagation, not different delays at the recording stations caused by irregular geology. In this work we assume constant rupture velocity implying that the time shifting parameter is associated with each recording station. Then instead of fitting the recorded data with theoretical data $\phi_{ij}(t)$, we can use $\phi_{ij}(t-\tau_i)$, where τ_i is unknown shift in time. Here 'i' refers to the ith station and τ_i is the same for all $\phi_{ij}(t)$ (all subfaults), due to the assumed constant rupture velocity. This model is different from that of Olson and Apsel who, through multiple slipping of subfaults, model variable dislocation velocities. Our optimization of the time shifts is associated with the effects of the propagation path which should be different for each station.

To derive the mathematical foundation of the proposed method, the LSQ system, consider equation (9) in a more abstract way. For simplicity only one station is considered in the fitting. Then the LSQ system can be derived by requiring that the residual error

$$\varepsilon(t)=\sum_{1}^{K} D_j\phi_j-f \tag{10}$$

be orthogonal with respect to the set of the functions $\{\phi_j(t)\}\, j=1,\ldots,J$, where $\phi_j(t)$ are the synthetics of the jth unit dislocation. The orthogonality condition leads to the system of equations,

$$\sum_{k}^{J}(D_k\phi_k-f,\phi_j)=0, \qquad j=1,2,\ldots J \tag{11}$$

where (ϕ_k, ϕ_j) is the scalar product in the set of functions $L_2(0, T)$.

Looking at the problem this way, one recognizes the method of weighted residuals, where the weighting functions are $\phi_j(t)$. These functions, as members of the vector space $L_2(0, T)$, span a linear subspace $Y\subset L_2(0, T)$. Hence (11) also means that the residual error has to be orthogonal to the subspace Y or $\varepsilon(t)\in Y^{\perp}$. It is known that for $\varepsilon(t)$ to be orthogonal to Y it is sufficient that $\varepsilon(t)$ be orthogonal to a set of base vectors of Y. If the set of functions $\{\phi_j(t)\}_1^J$ is linearly independent, then $\{\phi_j\}_1^J$ can be considered as the base. For the full treatment and discussion of the set $\{\phi_j\}_1^J$, one is referred to Jordanovski *et al.*[9]. We shall only point out that the physical similarity of the functions $\{\phi_j\}_1^J$ is one possible reason for the inversion instability.

Instead of using the set of functions $\{\phi_j(t)\}_1^J$ as a base in the $Y\subset L_2(0, T)$, one may choose a different set $\{\psi_j(t)\}_1^K$, in the residual method, to derive the LSQ system. For further numerical treatment it is very convenient to take for the new base a set of orthogonal functions such as sines and cosines. It is known that any function $g(t)\in L_2(0, T)$ can be represented by its discrete Fourier series:

$$g(t)=\sum_{k=1}^{\infty}\left\{g_s^k\sin\frac{2\pi}{T}kt+g_c^k\cos\frac{2\pi}{T}kt\right\}. \tag{12}$$

Expanding each record $f_i(t)$ and synthetics $\phi_{ij}(t)$ in terms of $\sin(2\pi/T)kt$ and $\cos(2\pi/T)kt$.

$$\begin{aligned} f_i(t)&=\sum_{k=1}^{\infty}\left\{b_i^k\sin\frac{2\pi}{T}kt+d_i^k\cos\frac{2\pi}{T}kt\right\}\\ \phi_{ij}(t)&=\sum_{k=1}^{\infty}\left\{S_{ij}^k\sin\frac{2\pi}{T}kt+C_{ij}^k\cos\frac{2\pi}{T}kt\right\}\end{aligned} \tag{13}$$

where

$i=1,2,\ldots I$ number of stations

$j=1,2,\ldots J$ number of unknown dislocations

one can form the equivalent LSQ system, after taking sufficiently large $k=K$

$$A\vec{D}=\vec{f} \tag{14}$$

where

$$\vec{f}=\{b_1^1, d_1^1, b_1^2, d_1^2,\ldots, b_I^1, d_I^1,\ldots, b_I^K, d_I^K\} \tag{15}$$

$$\vec{a}_J^T=\{S_{ij}^1, C_{ij}^1, S_{ij}^2, C_{ij}^2,\ldots, S_{Ij}^1, C_{Ij}^1,\ldots, S_{Ij}^K, C_{Ij}^K\}. \tag{16}$$

From the numerical standpoint, there is no difference in solving (9) and (14), but this LSQ problem enables us to include unknown time shift in the optimization.

One can write the series expansion, equation (13), for $\psi_{ij}(t+\tau_i)$. After some calculations, the relation between new coefficients in this discrete Fourier series and the previous series is given by

$$\begin{bmatrix} S_{ij}^k(\tau_i)\\ C_{ij}^k(\tau_i)\end{bmatrix}=R_i^k\begin{bmatrix} S_{ij}^k(0)\\ C_{ij}^k(0)\end{bmatrix}, \tag{17}$$

where $(S_{ij}^k(\tau_i), C_{ij}^k(\tau_i))$ are the kth pair of discrete Fourier coefficients of $\psi_{ij}(t+\tau_i)$ function, and $(S_{ij}^k(0), C_{ij}^k(0))$ are the kth pair of discrete Fourier coefficients of $\psi_{ij}(t)$, and

$$R_i^k=\begin{bmatrix}\cos\omega_k\tau_i & -\sin\omega_k\tau_i\\ \sin\omega_k\tau_k & \cos\omega_k\tau_i\end{bmatrix} \tag{18}$$

when $\omega_k=2\pi k/T$. The transformation mapping given by the matrix R_i^k is unitary and orthogonal and represents a rotation through an angle $\omega_k\tau_i$. If $\tau_i\ll 1$ then for small ω_k the rotation matrix R_i^k is close to the identity matrix. Therefore, the optimization for small τ_i in lower frequency bands does not give much advantage. However, for the higher frequencies even small τ_i can significantly change the coefficients $(S_{ij}^k(0), C_{ij}^k(0))$ and consequently the matrix A in equation (14). Clearly, the optimization of τ_i

will result in a nonlinear LSQ problem, and to solve it one will need to use one of the methods developed for nonlinear optimization. In what follows it is shown that this nonlinear problem can be transformed into two linear least squares problems.

Since the mapping (17) is linear, the new LSQ system matrix can be obtained as follows

$$A(\vec{\tau}) = R(\vec{\tau}).A \tag{19}$$

where

$$R = \begin{bmatrix} R_1^1 & & & & & & & \\ & R_1^2 & & & & & 0 & \\ & & \ddots & & & & & \\ & & & R_1^K & & & & \\ & & & & \ddots & & & \\ & & & & & R_I^1 & & \\ & 0 & & & & & R_I^2 & \\ & & & & & & & \ddots \\ & & & & & & & & R_I^K \end{bmatrix} \tag{20}$$

and

$$\vec{\tau} = (\tau_1, \tau_2, \ldots \tau_I).$$

Each submatrix R_i^k in (20) is given by (17) where k corresponds to the kth sine or cosine term, $k = 1$ to K and i corresponds to the ith recording station. The vector $\vec{\tau}$ contains the unknown time shift parameters associated with different recording stations. The new LSQ system is

$$R(\vec{\tau})A\vec{D} = \vec{f} \tag{21}$$

or due to unitary and orthogonal properties of R,

$$A\vec{D} = R^T(\vec{\tau})\vec{f}. \tag{22}$$

Equation (22) is the final form of the LSQ model in this application. Note that (22) means that instead of having synthetics shifted by τ_i, we shift the measured record by $-\tau_i$. The problem is still nonlinear, but now the nonlinear part is on the right-side and this enables one to perform the transformations on matrix A only once. For example, if one uses the method of damped least squares, one has to perform only one singular value decomposition of A. This significant saving in computational time enables us to represent the right hand side of (22) in the following form

$$R^T\vec{f} = \sum_{i=1}^{I}\left(\sum_{\tau=\tau_1}^{\tau=\tau_T} z_i^\tau \vec{b}_i^\tau\right) \tag{23}$$

where

$$[\vec{b}_i^\tau]^T = \{0, 0, \ldots 0, b_i^1(\tau), d_i^1(\tau), \ldots b_i^K(\tau), d_i^K(\tau), \ \ldots, 0 \ldots\} \tag{24}$$

and τ takes on discrete values on the interval $(0, T)$, not necessarily at equal intervals $\Delta\tau$. Thus for each $\tau\varepsilon(0, T)$ and for each station a new vector $\vec{b}_i^\tau$ is generated by shifting the data of the corresponding station by $-\tau$. This is done by transformation (17) and from the computational point of view is not time consuming. The Fourier components of the vector b_i^τ which do not belong to the station i are set to zero. The total number of such vectors is equal to the number of stations times the number of discrete values of τ_i in the interval $(0, T)$.

Since only one combination of $\tau_i, i = 1, 2, \ldots, I$ will minimize (22) one can see the nature of the new unknown vector $\vec{z}$,

$$\vec{z}^T = \{z_1^{\tau_1}, z_1^{\tau_2}, \ldots, z_1^{\tau_T}, \ldots, z_I^{\tau_1}, z_I^{\tau_2}, \ldots, z_I^{\tau_T}\}. \tag{25}$$

The components of vector $\vec{z}$, can be only zero or one. For the components belonging to the same station only one component can be equal to one, while the rest are equal to zero. The next expanded LSQ system then becomes

$$A\vec{D} = \sum_{i=1}^{I}\left(\sum_{\tau=\tau_1}^{\tau=\tau_T} z_i^\tau \vec{b}_i^\tau\right) \tag{26}$$

or

$$A\vec{D} = B\vec{z}. \tag{27}$$

The problem is now linear in variables $\vec{D}$ and $\vec{z}$.

To solve (26) we use the singular value decomposition method and replace A by USV^T[10]. Hence (27) can be written in the form

$$[U_1 : U_2]\begin{bmatrix} S & 0 \\ 0 & 0 \end{bmatrix}\begin{bmatrix} V_1^T \\ V_2^T \end{bmatrix}\vec{D} = B\vec{z} \tag{28}$$

or

$$\begin{bmatrix} S & 0 \\ 0 & 0 \end{bmatrix}\begin{bmatrix} V_1^T \\ V_2^T \end{bmatrix}\vec{D} = \begin{bmatrix} U_1^T B \\ U_2^T B \end{bmatrix}\vec{z} \tag{29}$$

where $[U] = [U_1 : U_2]$ and

$$V^T = \begin{bmatrix} V_1^T \\ V_2^T \end{bmatrix}$$

are orthogonal matrices. Then for a given $\vec{z}$, the solution of (29) is given by

$$SV_1^T\vec{D} = U_1^T B\vec{z} \tag{30}$$

and the error is

$$\text{Error} = \|U_2^T B\vec{z}\|. \tag{31}$$

The final error is a function of $\vec{z}$. Therefore to minimize the error (31) one has to solve the linear least square problem given by

$$U_2^T B\vec{z} = 0 \tag{32}$$

where $\vec{z}$ is subjected to the conditions after equation (25).

This type of problem is known in the theory of integer optimization as a quadratic zero–one programming[13,4,3]. However, the problem that we have here is uncommon due to the special constraints imposed on the vector $\vec{z}$. To the authors knowledge, there is no known general method for a straightforward solution for this type of problem.

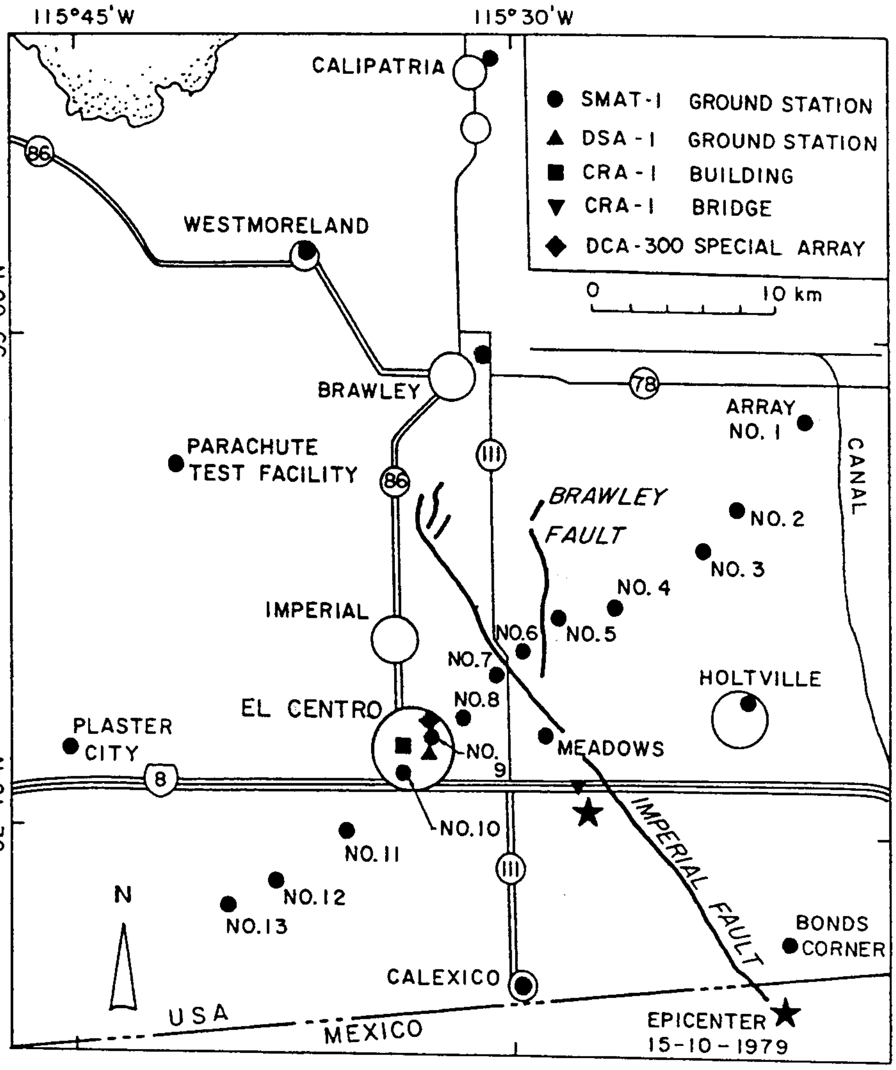

Fig. 2. Strong-motion stations in Imperial Valley, California

A common method used to solve the problem (32) is one of exhaustive search. By testing all possible combinations of the vector $\vec{z}$, the solution can be obtained. However, if the dimension of $\vec{z}$ is large the number of combinations becomes large so that in any reasonable computational time, it is not possible to check all combinations. The method that has been used here is an optimization of the exhaustive search procedure with respect to the computational time.

Singular value decomposition of matrix $U_2^T B$ in equation (32), yields the following LSQ system

$$\tilde{U}\tilde{S}\tilde{V}^T\vec{z}=0 \tag{33}$$

or

$$\tilde{S}\tilde{V}^T\vec{z}=0. \tag{34}$$

The dimension of the matrix $\tilde{S}\tilde{V}^T$ is of the same order as that of the vector $\vec{z}$. Considering the special requirements that vector $\vec{z}$ has to meet, $\vec{z}$ will be written in the following form

$$\vec{z}^T=\{\vec{z}_1^T, \vec{z}_2^T, \ldots, \vec{z}_I^T\} \tag{35}$$

where $\vec{z}_i^T$ is associated with the ith station. Similarly the matrix $\tilde{S}\tilde{V}^T$ can be partitioned into I submatrices as follows

$$[Q_1, Q_2, \cdots Q_I]\begin{bmatrix} \vec{z}_1 \\ \vec{z}_2 \\ \vdots \\ \vec{z}_I \end{bmatrix}=0. \tag{36}$$

Solution of (37) means, choosing one column vector from each of the Q_i such that the norm of their sum is minimum. The algorithm used in the numerical realization is the following.

(a) First one vector column is chosen as a starting vector, for example, the first column of the matrix Q_1. This means that the first component of the vector $\vec{z}_1$ is one and all other components of $\vec{z}_1$ are zero. Obviously the error is different from zero.
(b) In the next step one scans over all other columns in the rest of the matrices Q_i, excluding Q_1. The criterion for obtaining the second vector is either to reduce the

previous error or to increase it by the least possible amount.

(c) After the second vector is chosen one scans for the next vector over the rest of Q_i. This procedure continues until all submatrices Q_i have been used.

Since the iteration procedure usually depends on the initial point (in our case initial column vector), the final solution is not necessarily the global minimum. Therefore, the above procedure is repeated using each column of the starting submatrix as initial vector. The method was tried successfully on several theoretical examples. These examples consisted of generating data through linear combination of harmonic functions with known ω_K and τ_i and fitting these data by the same combination of harmonic functions, but now $\tau_i = 0$ for $\forall i$.

Although the proposed algorithm is based on the searching approach, its advantage lies in significant reduction in the number of combinations that have to be considered. For example, in the following case study, the number of stations is eight ($I = 8$) and each vector $\vec{z}_i$ has ten elements, so that all possible combinations add up to

$$N = 10^8$$

while with the above algorithm $N = 22\,440$.

By solving for unknown time shifts, one can substitute the vector $\vec{z}$ into equation (31) and solve for $\vec{D}$.

DISCUSSION

The above proposed algorithm has certain limitations. To obtain the LSQ system in terms of vector $\vec{z}$, one must associate unknown time shifts with the recording station. This means that at this stage this algorithm does not consider repeated slips for different subfaults. To include that possibility in the LSQ model of source inversion one can use the approach of Olson and Apsel[12]. However, even with their approach implemented, one will still require the shifting optimization with respect to the recording stations.

In choosing the time interval $(0, T)$, over which the unknown shifts are searched it is seen that by increasing this interval will increase the dimension of vector $\vec{z}$. This can be avoided by looking for the reference times in the recorded and synthetic data with phases which are clearly identifiable.

Table 1. Parameters of the model used in the inversion

Strike	N37W
Dip	90°
Slip	180°
Epicentre	32.63°N, 115.33°W
Rupture velocity	2.5 km/sec
Rise time	0.8 sec
Length	40 km
Width	10.4 km
Depth	10.5 km
P-velocity	5 km/sec
S-velocity	3 km/sec

Table 2. List of the stations used in this example

Station name	Estimated S-arrival	Code
El Centro #5	5.0 sec	EL05
El Centro #8	5.0 sec	EL08
Bonds Corner	2.4 sec	ELBC
El Centro #11	5.0 sec	EL11
Calexico	3.4 sec	ELCA
El Centro #4	4.7 sec	EL04
El Centro #2	5.0 sec	EL02
El Centro #1	5.0 sec	EL01

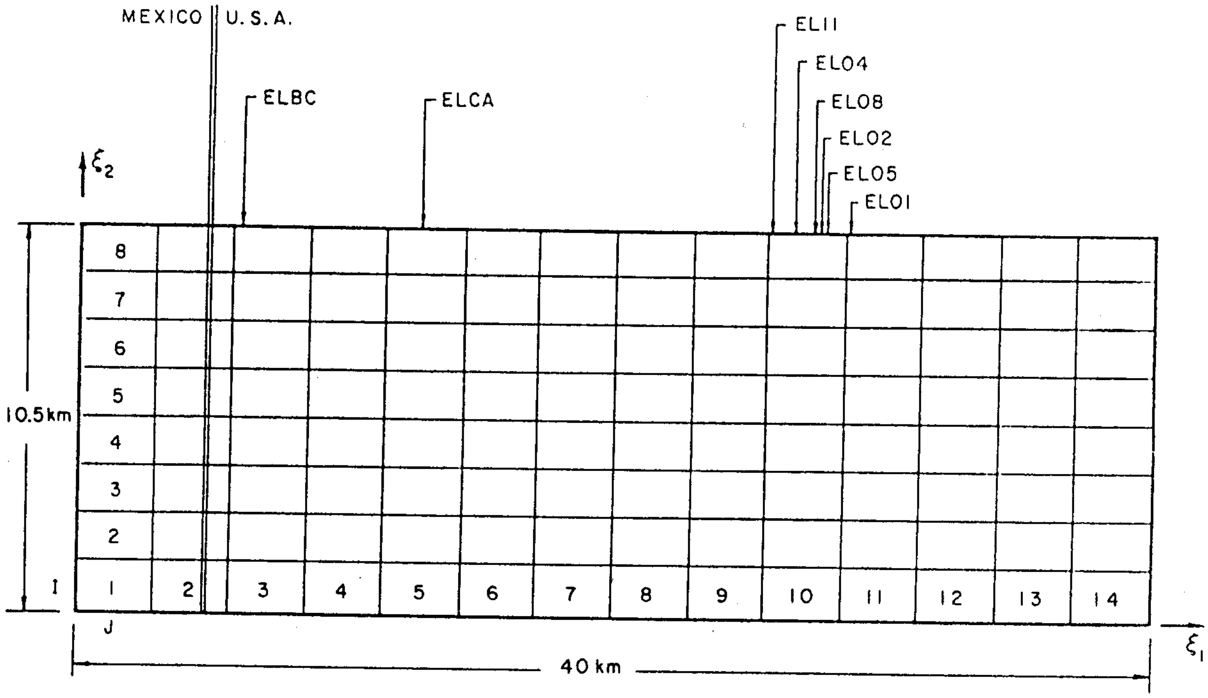

Fig. 3. Schematic representation of the fault and subfaults, together with stations' projections on the fault

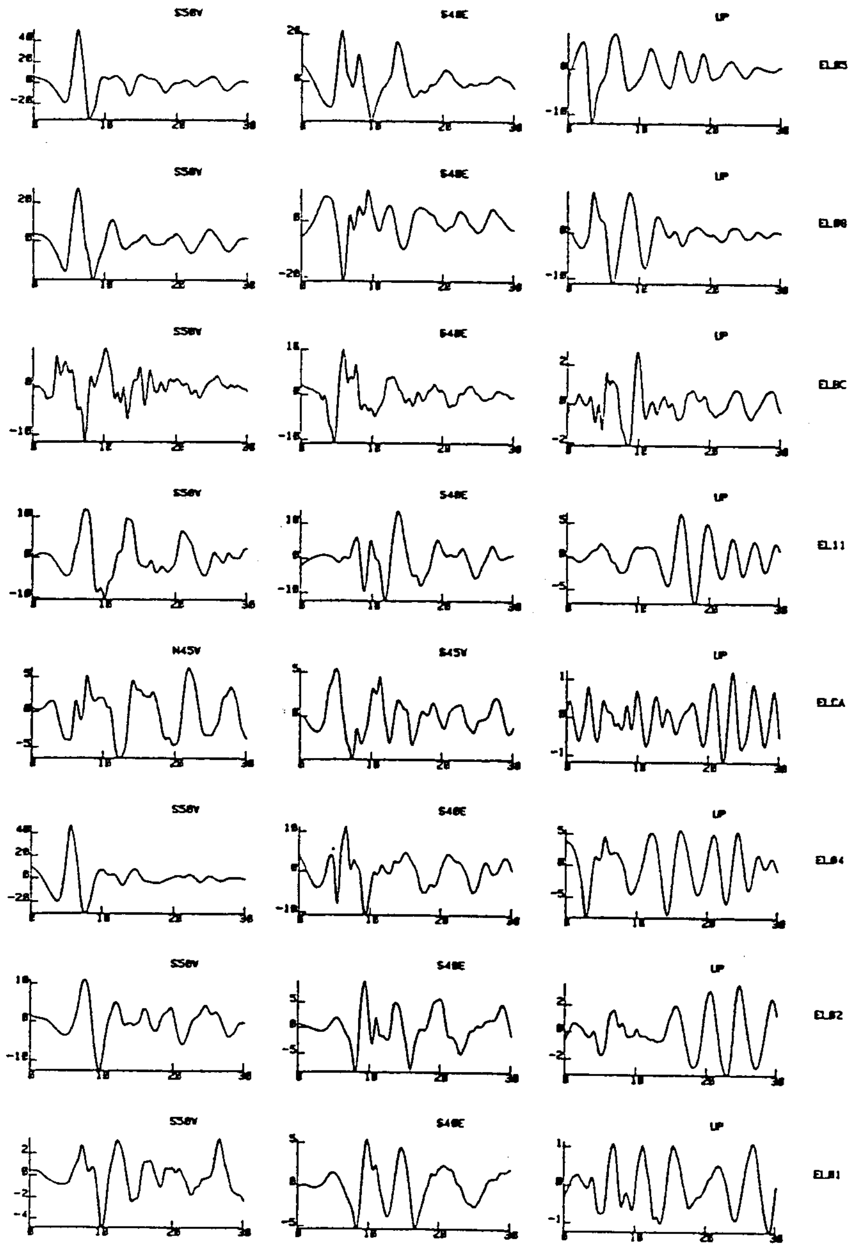

Fig. 4. Strong-motion displacements used in the inversion analysis

It is shown that shifting synthetic motions by τ_i is equivalent to shifting the recorded data by $-\tau_i$. It could happen that τ_i is such that the reference point for collocation is in negative time for the recorded data. Physically at that time the recorded data are zero but due to the representation of the data by discrete Fourier series and its properties, the data is periodically repeated with periods T. To avoid this possible error one can put enough zeros at the end and at the beginning of the recorded data to cover the maximum expected time shift.

The method proposed here still belongs to the group of trial and error procedures, but its form significantly reduces the number of the required trials. However, the efficiency of the method should not be considered out of the context of the whole inversion problem. The fact that one requires only one singular value decomposition of matrix A, and that the shifting of the recorded data for $-\tau_i$ can be efficiently programmed by the scheme using equation (17) and that the optimization model for $\vec{\tau}$ is a simple LSQ linear problem, all significantly save the computer time in favour of the search algorithm. The proposed method is thus much more economical than the trial and error procedure used in the very beginning of the inversion[6].

CASE STUDY: IMPERIAL VALLEY 1979 EARTHQUAKE

The Imperial Valley, California, earthquake of 1979 is taken here as an example to demonstrate the effects of the time shifting optimization. This earthquake has been the subject of many investigations[12,6,1,9] More than 40

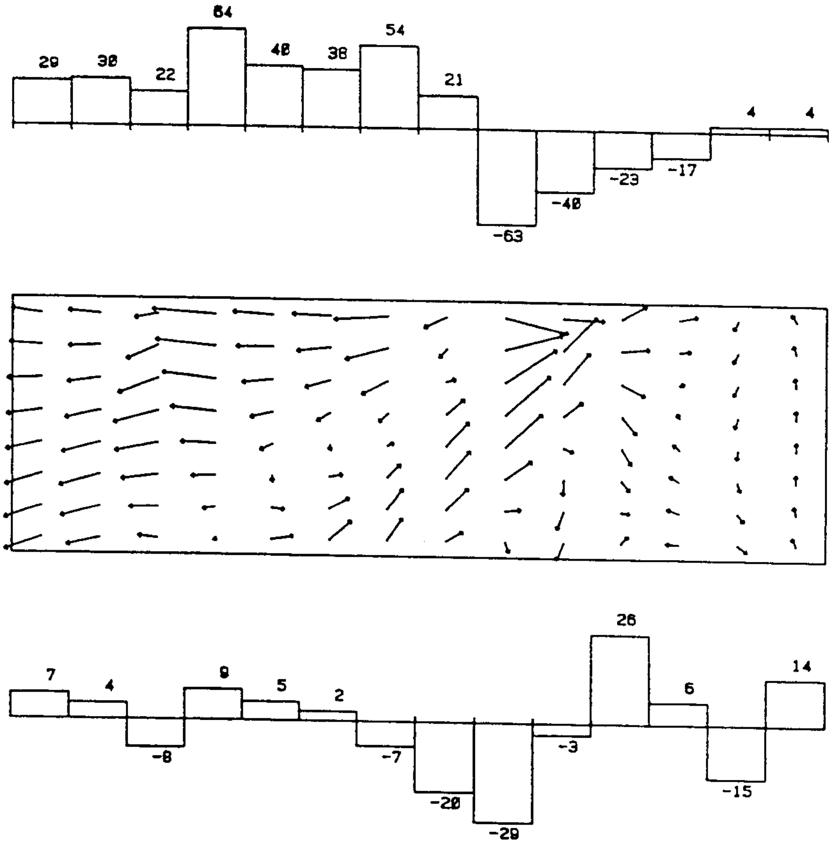

Fig. 5. Dislocation vectors (damping parameter $\alpha = 0.02$, see Jordanovski et al.[9]*) without shifting optimization. Top and bottom figures represent, respectively, the right lateral and vertical offsets in cm*

strong-motion instruments in the United States and in Mexico recorded the near-field ground acceleration at distances less than 35 km from the Imperial fault, Fig. 2. Since the subject of this paper is not the complete inversion of the Imperial Valley earthquake source, in what follows we present only a brief review of relevant data for illustration of the shifting optimization.

In Table 1 the parameters of the model used to form subfaults with dimensions 3×2 km the LSQ system are listed. Thus the fault was modelled by a plane divided into 120 subfaults (Fig. 3). In the process of inversion, eight stations have been used, Table 2. In Fig. (4) the time histories of the recorded displacements at these eight strong-motion stations are presented. The Haskell's dislocation time function and Green-tenzor for the full space have been used to calculate synthetic displacements. For the solution of the LSQ system the damped least square algorithm is used to avoid instability and to obtain physically acceptable results. For the purpose of comparison the following solutions are presented: (a) dislocation vectors calculated without the time shifting optimization (Figs 5 and 6) and (b) dislocation vectors with the time shifting optimization (Figs 7 and 8). The optimal τ_i are given in the Table 3. Figures 5 and 7 show dislocation vectors at the centre of each subfault. Figures 6 and 8 show comparison between the recorded and the calculated displacement data. All displacement data are scaled to 40 cm maximum value.

The top and bottom graphs in Figs 5 and 7 represent the amount of the final horizontal and vertical surface movement calculated from the model. Positive values of the surface displacement correspond to the right lateral faulting. For the vertical motions, the west side goes up relative to the east side for positive motion. The field measurements show that the motion on the Imperial fault was right lateral with the west side going up and with most of the faulting at some 30 km north from the epicentre. In light of this information one can see the important differences between the inversion model with and without the time shifting optimization. While the improvement is not noticeable in the fitting of the displacement in Figs 6 and 8, the effect of time shifting optimization is significant for the dislocation vectors, Figs 5 and 7. While the dislocation vectors and their values in the case with time shifting resemble and are in good agreement with other independent observations, the inversion model, without shifting, shows physically unrealistic dislocations which are not in agreement with the observations. For example the large dislocation is obtained in the beginning of the fault resulting in the large surface displacements in the southeastern end of the Imperial fault, which is contrary to the field observations. The other unrealistic result is very random behaviour of the dislocation vectors. Obviously, this model should be rejected although the fitting of the displacement data appears to be acceptable. It was also shown by Olson and Apsel[12], that a good match between the recorded and the synthetic data can be achieved without any time shifting optimization and regularization (damped inversion), but that the resulting dislocation vectors are physically unacceptable. Hence in

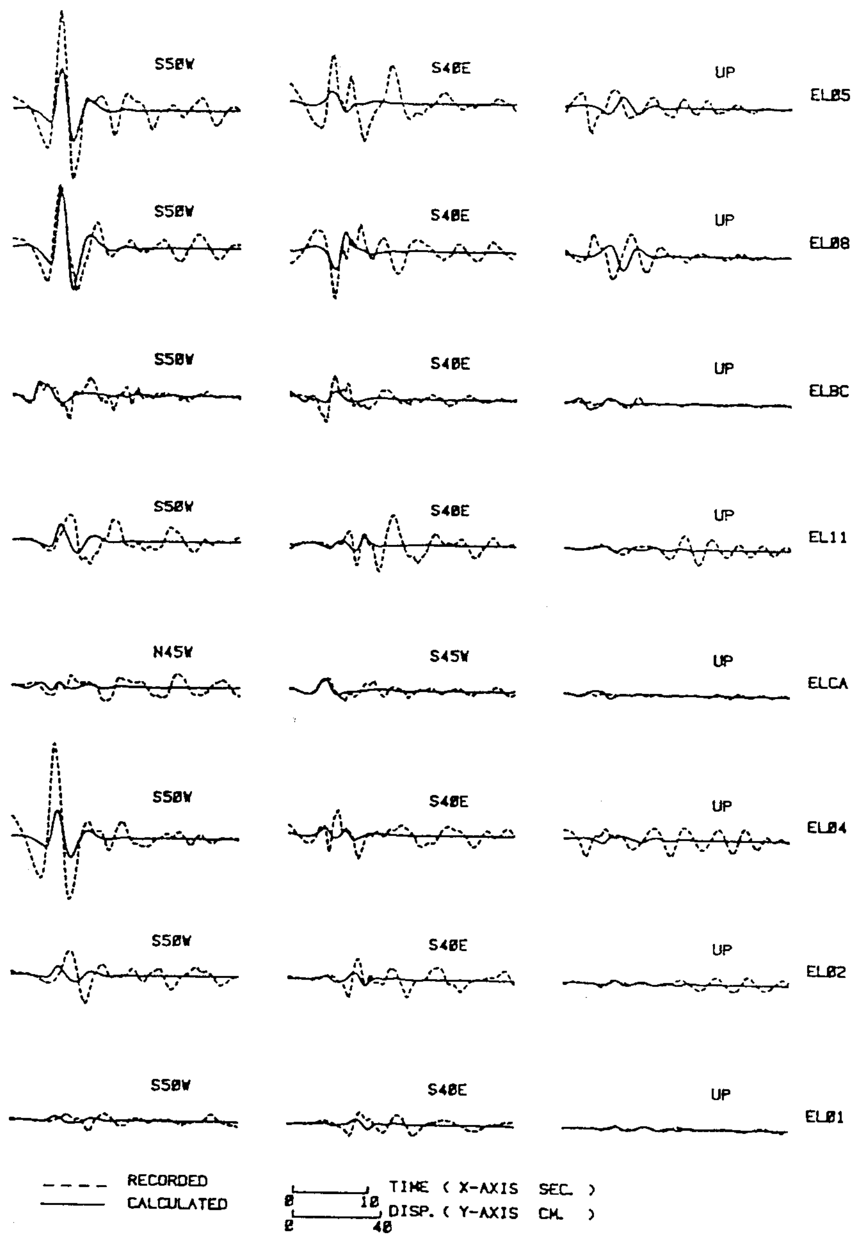

Fig. 6. Comparison between recorded and calculated displacements corresponding to the dislocation solution given in Fig. 5

the earthquake source inversion more weight must be given to the dislocation vectors and, as it is illustrated here, to the time shifting optimization.

The aim of this paper is not to suggest that the example presented here represents the best source mechanism solution, for the Imperial Valley 1979 earthquake, but to illustrate the degree of improvement that can be expected by incorporating the time shifting optimization at each recording station. The final solution is affected by many other details in the analysis, starting from the parametrization of the model, up to the numerical methods used in the process of solution, where the time shifting optimization is only one important step in the inversion process.

CONCLUSIONS

(1) The quality of the LSQ solution, involving inversion of the dislocation amplitudes in earthquake source mechanism studies can be improved by considering an additional parameter which represents the optimum time shift between the recorded data at each station and the synthetic motions. This has been illustrated for the Imperial Valley, California earthquake of 1979.

(2) The nonlinear LSQ problem with time shifts has been transformed into another LSQ problem with the nonlinear part on the right side of the equation. This problem can be linearized and solved by the method of exhaustive search. Optimization of this method is presented resulting in significant reduction of the required computer time.

(3) The dimension of the time shifting vector depends on the time interval $(0, T)$ in which the time shifts τ_i are sought and on the chosen sampling rate $\Delta\tau_{i+1} - \tau_i$.

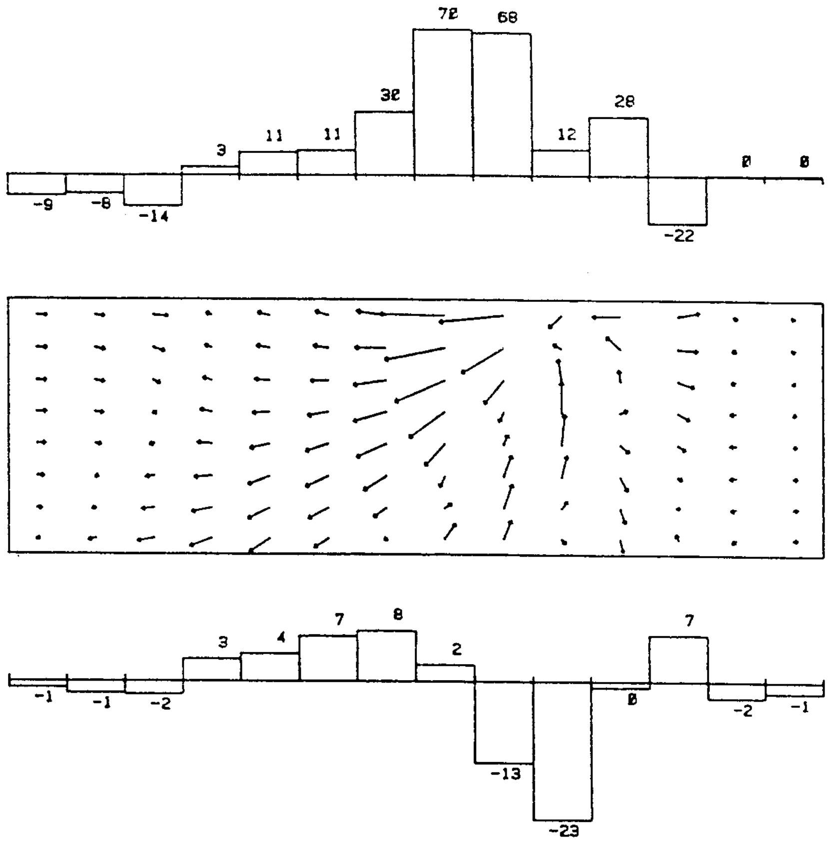

Fig. 7. Dislocation vectors (damping parameter $\alpha = 0.02$, see Jordanovski et al.[9]*) with shifting optimization. Top and bottom figures represent, respectively, the right lateral and vertical offsets in cm*

Table 3. Optimal shifting parameters

Station code	Optimal shift τ_i in seconds
S05	1.2
S08	1.0
SBC	0.0
S11	0.0
SCA	0.0
S04	1.4
SO2	0.0
SO1	0.0

We note that $\Delta\tau$ should not be too small since this will move the rotation matrix close to unity.

REFERENCES

1 Archuleta, R. J. A faulting model for the 1979 Imperial Valley earthquake, *Jour. Geoph. Res.*, 1984, **89**(B6), 4559–4585

2 Burridge, R. and Knopoff, L. Body force equivalent for seismic dislocation, *Bull Seism. Soc. Amer.*, 1964, **54**(6), 1875–1888

3 Greenberg, H. *Integer Programming*, Academic Press, New York, 1971

4 Hansen, P. Quadratic zero–one programming by implicit enumeration, in *Numerical Methods of Nonlinear Optimization*, edited by F. A. Lootsma, Academic Press, London, 1972, 265–278

5 Hartzell, S. H. and Helmberger, D. Strong-motion modeling of the Imperial Valley earthquake of 1979, *Bull. Seism. Soc. Amer.*, 1982, **72**(2), 571–596

6 Hartzell, S. H. and Heaton, T. H. Inversion of strong ground motion and teleseismic wave form data for the fault rupture history of the 1979 Imperial Valley, California, earthquake, *Bull. Seism. Soc. Amer.*, 1983, **73**(6), 1553–1583

7 Haskell, N. A. Elastic displacement in the near-field of a propagating fault, *Bull. Seism. Soc. Amer.*, 1969, **59**(2), 905–908

8 Johnson, C. E., Rojahn, C. and Sharp, R. V. The Imperial Valley, California earthquake, October 15, 1979, *U.S. Geol. Surv. Prof. Pap.*, 1254, 1–451

9 Jordanovski, L. R., Trifunac, M. D. and Lee, V. W. Investigation of numerical methods in inversion of earthquake source, *Dept of Civil Eng Report No. 86-01*, Univ. Southern California, Los Angeles, 1986

10 Lawson, C. L. and Hanson, R. J. *Solving Least Squares Problem*, Prentice-Hall, Inc., Englewood Cliffs, New York, 1974

11 Maruyama, T. On the first equivalent of dynamic elastic dislocation with reference to the earthquake mechanism, *Bull. of Earthq. Res. Inst.*, **41**, 467–468

12 Olson, V. H. and Apsel, R. J. Finite faults and inverse theory with applications to the 1979 Imperial Valley Earthquake, *Bull. Seism. Soc. Amer.*, 1982, **72**(6), 1969–2001

13 Rao, S. S. *Optimization, Theory and Application*, Wiley Eastern Limited, New Delhi, 1979

14 Trifunac, M. D. and Hudson, D. E. Laboratory evaluation and instrument corrections of strong motion accelerographs, *EERL 70-04*, California Institute of Technology, Pasadena, 1970

15 Trifunac, M. D. Zero base-line correction of strong motion accelerograms for instrument response, *Bull. Seism. Soc. Amer.*, 1971, **61**, 1201–1211

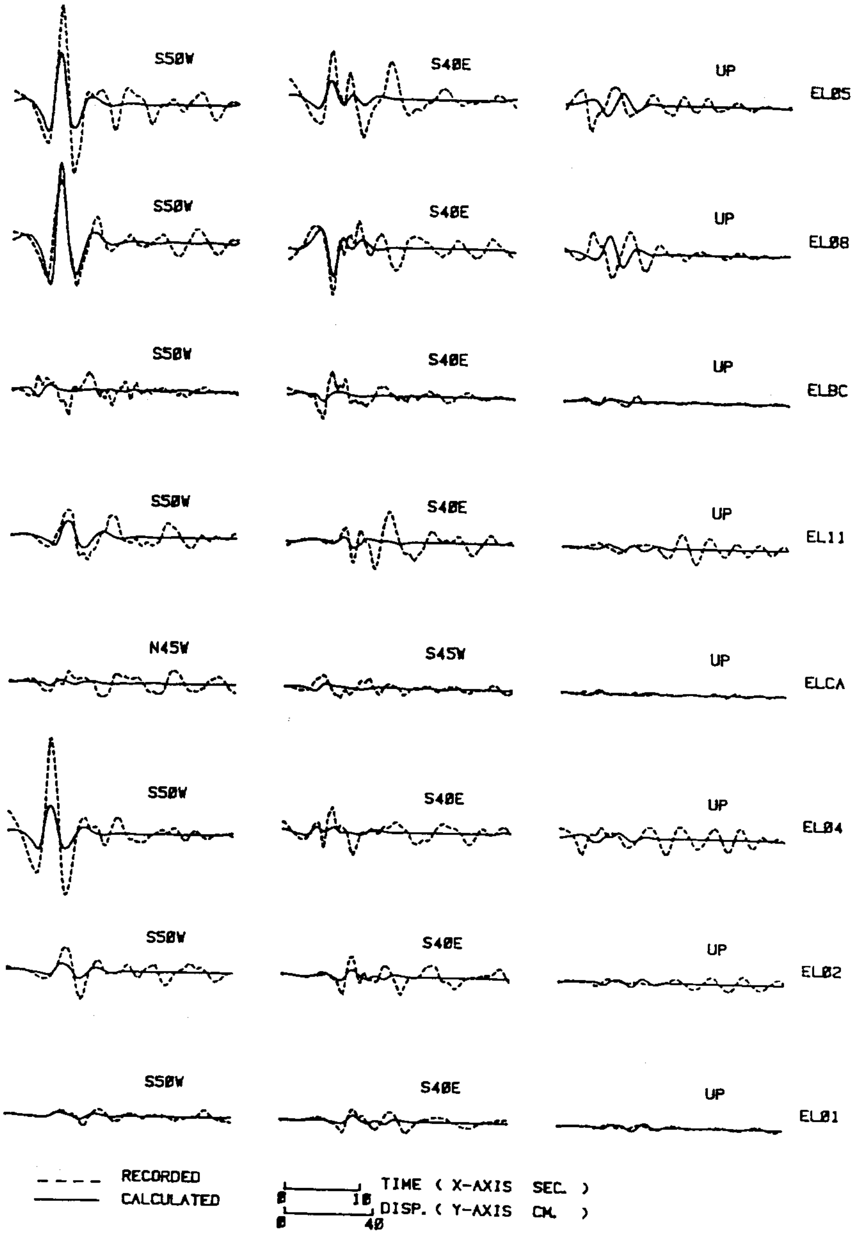

Fig. 8. Comparison between recorded and calculated displacements corresponding to the dislocation solution given in Fig. 7

16 Trifunac, M. D. A note on correction of strong motion accelerograms for instrument response, *Bull. Seism. Soc. Amer.*, 1972, **62**, 401–409

17 Trifunac, M. D. A three-dimensional dislocation model for the San Fernando, California, earthquake of February 9, 1971, *Bull. Seism. Soc. Amer.*, 1974, **64**(1), 511–533

18 Trifunac, M. D. and Lee, V. W. A note on the accuracy of computed ground displacements from strong motion accelerograms, *Bull. Seism. Soc. Amer.*, 1974, **64**, 1209–1219

19 Trifunac, M. D. and Udwadia, F. E. Parkfield, California, earthquake of June 27, 1966: a three-dimensional moving dislocation, *Bull. Seism. Soc. Amer.*, 1974, **64**(3), 511–533